



Regular paper

Insights into the stress response and sulfur metabolism revealed by proteome analysis of a *Chlorobium tepidum* mutant lacking the Rubisco-like protein

Thomas E. Hanson¹ & F. Robert Tabita^{2,*}

¹Graduate College of Marine Studies and Delaware Biotechnology Institute, University of Delaware, Newark, DE 19711, USA; ²Department of Microbiology and Plant Molecular Biology/Biotechnology Program, The Ohio State University, Columbus, OH 43210-1292, USA; *Author for correspondence (e-mail: tabita.1@osu.edu; fax: +1-614-292-6337)

Received 30 December 2002; accepted in revised form 21 April 2003

Key words: green sulfur bacteria, Rubisco-like protein, stress response, sulfur oxidation

Abstract

A significant fraction of the proteome of *Chlorobium tepidum* is altered in a mutant strain of the green sulfur bacterium *C. tepidum* (Ω ::RLP) lacking the Rubisco-like protein (RLP). Additionally, a number of stress proteins display altered abundance or migration in strain Ω ::RLP, including a thioredoxin, a putative Hsp20 family chaperonin, and GroEL. Changes in protein abundance are closely correlated to mRNA abundance in the case of two other stress proteins, a thiol-specific antioxidant protein homolog (Tsa/AhpC) and an iron only superoxide dismutase (Fe-SOD). Strain Ω ::RLP is more resistant to hydrogen peroxide exposure than strain WT2321, providing evidence that the stress proteins are functional. Strain Ω ::RLP is also defective in thiosulfate oxidation, but is able to oxidize sulfide as well as the wild-type strain. Based on studies with periplasm-enriched extracts of strain Ω ::RLP, the loss of thiosulfate oxidation capability correlates with undetectable levels of the SoxY protein, a component of the predicted thiosulfate oxidation complex. These results provide further indications that sulfur oxidation capacity and the response to stress are linked in *C. tepidum*, with the RLP playing a major role.

Abbreviations: RLP – Rubisco-like protein; Sox – thiosulfate oxidation complex

Introduction

Ribulose 1,5-bisphosphate (RuBP) carboxylase/oxygenase (Rubisco) is the most abundant enzyme on earth (Ellis 1979) and is the key catalyst of the Calvin–Benson–Bassham (CBB) cycle of autotrophic CO₂ fixation in plants and a wide variety of bacteria (Tabita 1999). As a result of recent microbial genome sequencing efforts, two new types of Rubisco molecules have been recognized; these are the form III Rubisco's from archaea and the form IV Rubisco-like protein (RLP) sequences from bacteria and archaea. The form III proteins are *bona fide* Rubisco catalysts (Ezaki et al. 1999; Tabita 1999; Watson et al. 1999) but

the form IV proteins (RLPs) represent an interesting variation in that they both resemble and differ from *bona fide* Rubisco enzymes but do not catalyze RuBP-dependent CO₂ fixation (Hanson and Tabita 2001). These findings have greatly expanded our view of the diversity of this enzyme family. This paper describes recent insights revealed by proteomic and physiological studies using a mutant strain of the green sulfur bacterium *Chlorobium tepidum* (strain Ω ::RLP) that lacks the RLP.

RLP molecules are delineated from true Rubisco's on the basis of two criteria. First, RLP sequences form a distinct, coherent clade within phylogenetic trees constructed from alignments of form I, form

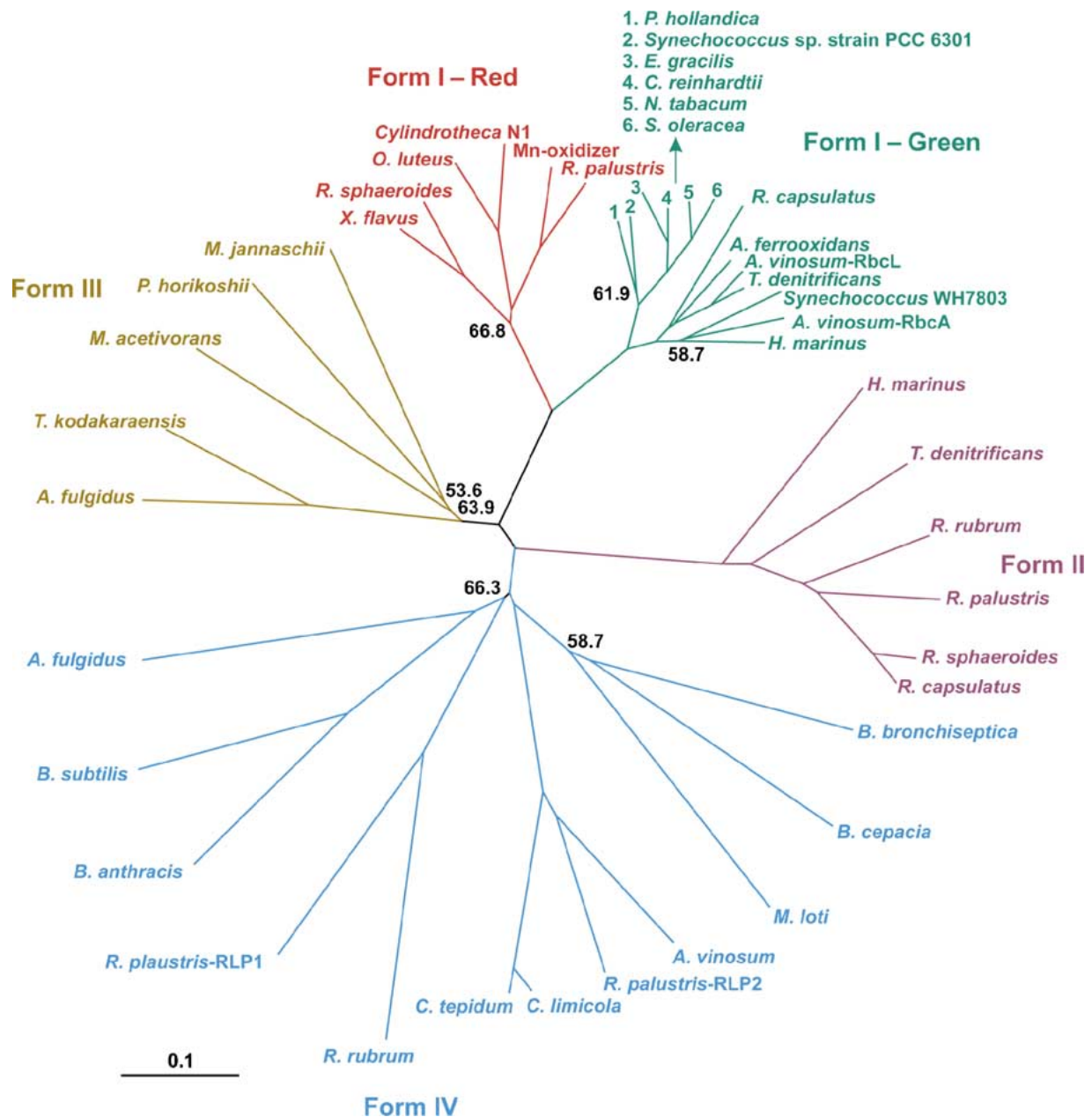


Figure 1. Unrooted neighbor joining phylogenetic tree showing the relationship of *bona fide* Rubisco sequences (form I – in red and green, form II – in purple, form III – bronze) and the RLP sequences (form IV – in cyan). Bootstrap values at the nodes indicate the percentage of times that particular node was present in 1000 trials. Only nodes with less than 70% bootstrap support are indicated. The scale bar represents 0.1 substitutions per site.

II and form III Rubisco molecules (Figure 1), with RLP sequences derived from a broad range of organisms (Table 1). Recently available sequences included in the tree reinforce the notion that the RLP's (form IV) are very diverse and contain at least one subgroup comprised of RLP's from the green sulfur

bacteria *C. tepidum* and *C. limicola*, along with RLP2 from the purple non-sulfur bacterium *R. palustris* and the RLP found in the purple sulfur bacterium *A. vinosum* (Figure 1). Aside from these four RLP molecules, which display ~60% amino acid sequence identity, the entire RLP family shares only

Table 1. Sequences used to construct the phylogenetic tree in Figure 1

Rubisco sub-family	Organism	Source/accession number
Form I – Red	<i>Xanthobacter flavus</i>	P23011
	<i>Rhodobacter sphaeroides</i>	P27997
	<i>Olisthodiscus luteus</i>	P14959
	<i>Cylindrotheca</i> sp. Strain N1	P24673
	Mn-oxidizing bacterium strain SI85-9A1	AAB41464
	<i>R. palustris</i>	DOE-JGI ^a
Form I – Green	<i>Synechococcus</i> sp. strain PCC 6301	P00880
	<i>Prochlorothrix hollandica</i>	P27568
	<i>Euglena gracilis</i>	NP_041936
	<i>Chlamydomonas reinhardtii</i>	P00877
	<i>Nicotiana tabacum</i>	P00876
	<i>Spinacia oleracea</i>	P00875
	<i>Rhodobacter capsulatus</i>	Q32740
	<i>Acidithiobacillus ferrooxidans</i>	AAD30508
	<i>Allochromatium vinosum</i> (RbcL)	P22849
	<i>Thiobacillus denitrificans</i>	Q56259
	<i>Synechococcus</i> sp. Strain WH 7803	P96486
	<i>A. vinosum</i> (RbcA)	P22859
<i>Hydrogenovibrio marinus</i>	Q59460	
Form II	<i>H. marinus</i>	Q59462
	<i>T. denitrificans</i>	Q60028
	<i>Rhodospirillum rubrum</i>	230725
	<i>R. palustris</i>	DOE-JGI
	<i>R. sphaeroides</i>	P29278
	<i>R. capsulatus</i>	P50922
Form III – Archaeal	<i>Archaeoglobus fulgidus</i>	NP_070466
	<i>Thermococcus kodakaraensis</i>	BAA33863
	<i>Methanosarcina acetivorans</i>	W. Metcalf ^b
	<i>Pyrococcus horikoshii</i>	NP_142861
	<i>Methanocaldococcus jannaschii</i>	NP_248230
Form IV – Rubisco-like	<i>C. tepidum</i>	TIGR ^c
	<i>C. limicola</i> f. sp. <i>thiosulfatophilum</i>	AAK14332
	<i>R. palustris</i> (RLP2)	DOE-JGI
	<i>A. vinosum</i>	BAB44150
	<i>Mesorhizobium loti</i>	NP_107406
	<i>Burkholderia cepacia</i>	Sanger ^d
	<i>Bordetella bronchiseptica</i>	Sanger
	<i>R. palustris</i> (RLP1)	DOE-JGI
	<i>A. fulgidus</i>	NP_070416
	<i>B. subtilis</i>	NP_389242
<i>B. anthracis</i>	TIGR	

^a United States Department of Energy-Joint Genome Institute, <http://www.jgi.doe.gov>.

^b Personal communication.

^c The Institute for Genomic Research, <http://www.tigr.org>.

^d The Sanger Centre, <http://www.sanger.ac.uk>.

~25%–30% overall sequence identity; moreover, individual RLP's are no more related to one another than they are to Rubisco's of forms I–III. These distinct

differences in sequence identity might indicate that there are multiple physiological roles for phylogenetically distinct RLP molecules.

The second criterion separating RLP from *bona fide* Rubisco is that all RLPs contain varying numbers of substitutions at residues that comprise known active site residues that are invariant in *bona fide* Rubisco molecules. In the case of the *C. tepidum* RLP, nine of nineteen active site residues have been replaced by non-conservative amino acid substitutions. Not surprisingly, no significant Rubisco activity was demonstrated by purified recombinant *C. tepidum* RLP or crude extracts of *C. tepidum* (Hanson and Tabita 2001).

The precise physiological role of most RLPs remains enigmatic. Studies on strain Ω ::RLP, a mutant of *C. tepidum* in which the RLP-encoding gene (*CT1772*) was inactivated, indicated that RLP may somehow be involved with sulfur metabolism and the response to oxidative stress. Studies on the RLP encoded by the *ykrW* gene of *B. subtilis* indicate a role for this protein in recycling of methylthioadenosine produced as a by-product of spermidine biosynthesis (Grundy and Henkin 1998; Murphy et al. 2002; Sekowska and Danchin 2002). However, *C. tepidum* RLP is unlikely to carry out the same function, consistent with the fact that the *B. subtilis* and *C. tepidum* sequences fall within different sub-groups of RLP molecules (Figure 1). The two proteins themselves are also not very similar and contain different patterns of substitutions at Rubisco active site residues. Furthermore, the recently completed *C. tepidum* genome does not encode orthologs of any of the other genes proposed to complete the methylthioadenosine recycling pathway (Eisen et al. 2002). Most convincingly, the pleiotropic phenotype exhibited by *C. tepidum* strain Ω ::RLP is exhibited under normal growth conditions while the *B. subtilis ykrW* mutant has to be highly starved for sulfur before a phenotype becomes apparent (Murphy et al. 2002; Sekowska and Danchin 2002). These observations bolster the hypothesis that subfamilies of RLPs, as delineated by phylogenetic comparisons, may carry out distinct physiological roles in their respective hosts.

In order to further characterize the physiological role of the *C. tepidum* RLP, we have undertaken comparative physiological and proteomics studies of the wild type strain WT2321 and strain Ω ::RLP. These studies have greatly extended earlier indications that oxidative stress responses and sulfur metabolism are perturbed in strain Ω ::RLP. For example, proteomic comparisons indicated that a large fraction of the *C. tepidum* protein profile was changed in strain Ω ::RLP.

In addition to the previously identified thiol-specific antioxidant protein superfamily (Tsa/AhpC) homolog and iron superoxide dismutase (Fe-SOD) (Hanson and Tabita 2001), additional stress response proteins were identified on the basis of their altered abundance or migration in strain Ω ::RLP. In two instances, protein abundance was shown to correlate with changes at the level of gene transcription. Most importantly, altered patterns of protein accumulation correlated with significant increases in the tolerance of strain Ω ::RLP to peroxide stress, reinforcing and extending initial observations that the RLP appears to affect the regulation of stress responses in *C. tepidum*. Finally, protein analyses of periplasm-enriched extracts in strain Ω ::RLP indicated that a predicted thiosulfate oxidation protein, SoxY (Friedrich et al. 2001; Quentmeier and Friedrich 2001; Eisen et al. 2002), correlated with defects in normal thiosulfate oxidation capacity. These results, taken together, suggest that RLP plays a central role in the physiology of *C. tepidum* and directly or indirectly affects stress responses and sulfur metabolism in this organism.

Materials and methods

Sequence alignments and phylogenetic tree construction

The sources of the sequences used to construct the phylogenetic tree in Figure 1 are listed (Table 1). Multiple sequence alignments and bootstrapped neighbor joining trees were constructed using ClustalX 1.8 (Thompson et al. 1997). Trees were visualized with TreeView 1.6.6 (Page 1996) and prepared for publication using Corel Draw 8 (Corel Corporation, Ottawa, Canada). The scale bar corresponds to 0.1 substitutions per site.

Strains and growth conditions

The construction of *C. tepidum* strain Ω ::RLP and the growth of *C. tepidum* wild type strain WT2321 and strain Ω ::RLP were described previously (Hanson and Tabita 2001). Cultures (20 ml) were grown in sealed 25 ml tubes (Bellco, Vineland, New Jersey) under a headspace of 95% N₂ + 5% CO₂ unless otherwise noted. *C. tepidum* growth was quantitated by following the protein content of cultures (Mukhopadhyay et al. 1999).

Two dimensional SDS-PAGE comparison of C. tepidum strains

Three autotrophic cultures each of *C. tepidum* strain WT2321 and strain Ω ::RLP were grown to mid-exponential phase ($100\text{--}120\ \mu\text{g protein ml}^{-1}$) and harvested by centrifugation at $7500 \times g$ for 5 min at room temperature. Cell pellets were stored at $-70\ ^\circ\text{C}$ until processing. At the desired time, cell pellets were resuspended in 0.5 ml cold lysis buffer (20 mM Tris-HCl, pH 7.5 + 10 mM MgCl_2 + 1 mM EDTA + 10 mM β -mercaptoethanol + 10% glycerol). Cells were lysed using a Heat Systems (Farmingdale, New York) model W-385 sonicator equipped with a microprobe tip. Samples were sonicated for 2 min using a 50% duty cycle, power setting = 3.5, while being cooled in an ice water bath. Cell debris was removed by centrifugation at $16,000 \times g$ for 5 min at $4\ ^\circ\text{C}$. Extracts were fractionated by ultracentrifugation at $150,000 \times g$ for 60 min at $4\ ^\circ\text{C}$. The supernatant from the ultracentrifugation was carefully removed and was designated the soluble fraction. The protein concentration in soluble fraction samples was determined with a modified Lowry protocol (Markwell et al. 1978).

Soluble fraction protein samples ($100\ \mu\text{g protein}$) were adjusted to 8 M urea + 1% CHAPS + 2 mM tributylphosphine + 0.2% BioLytes 3-10 + 0.001% bromophenol blue in a volume of $350\ \mu\text{l}$. Samples were applied to 17 cm ready strip pH 3-10 IPG strips (Bio-Rad) using the active rehydration program on a Protean IEF cell (Bio-Rad). Samples were focused for a total of 95,000 V h after 15 min of prefocusing at 250 V using the linear ramp program from 250 to 10,000 V.

SDS-PAGE on pre-cast Protean 8-16% gradient gels (Bio-Rad) was carried out after equilibrating focused IPG strips according to manufacturer's instructions. Gels were stained with a mass spectrometry compatible silver stain kit (Silver Stain Plus, Bio-Rad) and gel images collected using a FluorS MultiImager operated by PDQuest software Version 6.2.1 (Bio-Rad). Molecular mass and pI values for proteins were estimated by comparison to gels of 2D SDS-PAGE standards (Bio-Rad) separated under the same conditions as the samples. Gel images were processed, normalized and compared with PDQuest 6.2.1. For quantitative comparisons, a matchset was constructed from the six gel images corresponding to the soluble fractions of strain WT2321 and Ω ::RLP. Spot intensities were normalized using the 'total density in gel

image' method in PDQuest 6.2.1 and values for spot intensity are reported as parts per million (ppm) reflecting the contribution of each spot to the total pixel density present in the image.

Protein identification by mass spectrometry

Two-dimensional gels were run as above except that $400\ \mu\text{g}$ of soluble extract protein was loaded. After second dimension electrophoresis, gels were fixed in 50% ethanol + 10% acetic acid overnight followed by two 30 min washes in 50% methanol + 5% acetic acid. Staining was carried out with 0.25% Coomassie R-250 (Sigma, St. Louis, Missouri) dissolved in 50% methanol + 5% acetic acid. Gels were destained in 50% methanol + 5% acetic acid and stored in 5% acetic acid at $4\ ^\circ\text{C}$ until coring. Proteins identified as having altered abundance in the silver stained gels were cored using a robotic spot cutter (Bio-Rad) and cores were analyzed at The Ohio State University Campus Chemical Instrument Center. Proteins in gel cores were digested with modified sequencing grade trypsin (Promega, Madison, Wisconsin).

Following digestion, matrix assisted laser desorption/ionization time-of-flight (MALDI-TOF) was performed on a Reflex III mass spectrometer (Bruker, Bremen, Germany) operated in linear, positive ion mode with a N_2 laser. Laser power was used at the threshold level required to generate signal. Accelerating voltage was set to 28 kV. The instrument was calibrated with protein standards bracketing the molecular weights of the protein samples (typically mixtures of bradykinin fragment 1-5 and human adrenocorticotrophic hormone fragment 18-39 as appropriate (Fluka, St. Louis, Missouri). Salt buffers from the digestion samples were cleaned when necessary using ZipTips (Millipore, Bedford, Massachusetts) according to manufacturer's directions. α -Cyano-4-hydroxycinnamic acid (Fluka, St. Louis, Missouri) was used as the matrix and prepared as a saturated solution in 50% acetonitrile/0.1% trifluoroacetic acid (in water). Aliquots of $10\ \mu\text{l}$ of matrix and $2\ \mu\text{l}$ of sample were thoroughly mixed together; $0.5\ \mu\text{l}$ of this was spotted on the target plate and allowed to dry. MALDI-TOF spectra are monoisotopic masses and reported as $[\text{M} + \text{H}]^+$. The resulting mass profile was searched against databases using the Mascot search program (MatrixScience, London, UK) or manually matched to peptide mass profiles generated from known *C. tepidum* proteins or other protein sequences with the Peptide Mass program at the ExPASy WWW

server (<http://ca.expasy.org/tools/peptide-mass.html>). Profiles were generated as monoisotopic $[M + H]^+$ masses of tryptic derived peptides allowing up to one missed cleavage site per peptide.

When MALDI-TOF MS did not unambiguously identify a *C. tepidum* protein, samples of digested cores were further analyzed by capillary liquid chromatography nanospray tandem mass spectrometry (Nano-LC-MS/MS). Nano-LC-MS/MS was performed on a hybrid quadrupole time-of-flight mass spectrometer (Q-ToF II, Micromass, Wythenshawe, UK) equipped with an orthogonal nanospray source from New Objective, Inc. (Woburn, Massachusetts) operated in positive ion mode. The LC system was a Waters Alliance 2690 Separation Module (Waters, Milford, Massachusetts). Solvent A was water containing 50 mM acetic acid and solvent B was acetonitrile. Of each sample, 10 μ l was first injected on to the trapping column, which was then washed with solvent A. The injector port was switched to inject and the peptides were eluted off of the trap onto the column. A 10 cm, 50 μ m I.D. BioBasic C18 column packed directly in the nanospray tip was used for chromatographic separations. Peptides were eluted directly off the column into the Q-TOF system using a gradient of 3–80% B over 20 min, with a flow rate of 280 μ l/min with a pre-column split to about 500 nl/min. Total run time was 35 min. The nanospray capillary voltage was at 2.8 kV and cone at 55 V. The source temperature was maintained at 100 °C. Mass spectra were recorded using MassLynx 3.5 automatic switching functions. Mass spectra were acquired from mass 300 to 2000 Da every 1 s with a resolution of 8000 (FWHM). When the desired peak (using include tables) was detected at a minimum of eight ion counts, the mass spectrometer automatically switched to acquire CID MS/MS spectrum of the individual peptide. Collision energy was set dependent on charge state recognition properties. Sequence information from the MS/MS data was processed using the MassLynx 3.5 Biolynx software. Resulting spectra were searched against the NCBI non-redundant protein database using the Mascot Sonar MS/MS search program to identify the corresponding *C. tepidum* protein.

Quantitative reverse transcriptase PCR (RT-PCR) assay for mRNA quantitation

C. tepidum sequence data (Eisen et al. 2002) was obtained from The Institute for Genomic Research website (<http://www.tigr.org>). Primers were designed

with the aid of Gene Runner software Version 3.05. The following amplicons were used in this study for quantitation of mRNA levels by quantitative RT-PCR: A 117 bp section of gene *CT1492* encoding the Tsa/AhpC homolog was amplified using primer Tsa-RT-F (5'-TGCTCGGTTGCTCGGTTGAC-3') and primer Tsa-RT-R (5'-TGGTCTTGTTGATGTCGGAGATGA-3'). A 118 bp section of gene *CT1211*, encoding an iron only superoxide dismutase, was amplified using primer Sod-RT-F (5'-CGAAGGCACGCCATATGACG-3') and Sod-RT-R (5'-GTAGAAGCTGTGGTTCCATGCCTG-3'). Finally, a 118 bp section of gene *CT1551* encoding SigA, the presumed major housekeeping sigma factor (Gruber and Bryant 1998), was amplified using primer Sig-RT-F (5'-ACGAGGGCCATCAAGGAAGGT-3') and primer Sig-RT-R (5'-TGGCCACCGAAACCACGAA-3').

RNA was prepared from early to mid-exponential phase *C. tepidum* strain WT2321 and $\Omega::$ RLP cultures ($\sim 60 \mu$ g protein ml⁻¹) by a hot SDS:phenol extraction method (Tong et al. 1996) followed by LiCl precipitation (Ausubel et al. 1987). RNA samples were treated with RNase-free DNase I (Amplification grade, Invitrogen, Carlsbad, California) to minimize genomic DNA contamination. Reverse transcription reactions were carried out with a commercial kit (Omniscript RT, Qiagen, Valencia, California).

Quantitative PCR reactions (25 μ l) were performed on 1:10 diluted reverse transcription (+RT) reactions and -RT controls (for genomic DNA contamination) using the QuantiTect SYBR Green PCR kit (Qiagen). Data sets were collected on a BioRad iQ Real Time PCR System using iCycler Version 2.3.1370 software and analyzed using the same software. Fluorescein (10 nM in all reactions, Bio-Rad) was used to collect well correction factors prior to data acquisition. The cycling conditions were: 15 min at 95 °C (activation of *Taq* polymerase) + 90 s at 94 °C (well factor collection) followed by 45 cycles of 30 s at 94 °C, 30 s at 60 °C, and 60 s at 72 °C. Fluorescence signal data were collected during the 72 °C phase of each cycle. Melt curves from 95 °C to 56 °C in 0.5 °C increments, measuring fluorescence at each temperature, were collected for all samples following the last cycle.

All genes studied are present in the *C. tepidum* chromosome in single copy. Therefore, dilutions of CsCl purified (Ausubel et al. 1987) *C. tepidum* strain WT2321 genomic DNA were used to construct independent standard curves for each gene ranging from

50 to 5×10^7 copies per reaction with each point measured in triplicate. Efficiencies for amplification of each gene were similar based on the slopes of the standard curves. The standard curves were used to derive the copy number of each gene in three RNA samples from independent cultures of each strain. The copy number in each RNA sample was determined in triplicate. The derived copy number for either oxidative stress gene was divided by *sigA* transcript copy number resulting in an expression ratio, which normalizes for differences in RNA preparation and amplification efficiency between samples. These expression ratios are presented in Figure 5A. The *sigA* transcript copy number was found to be relatively constant (292 ± 107 copies per nanogram total RNA) across all samples, which may indicate it as a generally useful reference gene. The observed variance is likely due to differences in quality of individual RNA preparations.

T-tests (Microsoft Excel, two-sample, assuming unequal variance, $\alpha = 0.05$) were used to determine if the differences observed for transcript, activity and protein levels between strains WT2321 and $\Omega::RLP$ were statistically significant. The resulting *P*-values are noted (Figure 5A).

Oxidative stress resistance of C. tepidum strains

Resistance of *C. tepidum* strains to $400 \mu\text{M H}_2\text{O}_2$ was measured by a viable plate count assay. To quantitate viable cells, 0.1 ml samples taken from early exponential phase ($40\text{--}50 \mu\text{g protein ml}^{-1}$) cultures were immediately injected into sealed sterile 2.5 ml serum vials containing an atmosphere of 2.5% $\text{H}_2 + 97.5\%$ N_2 . Vials were quickly transferred into an anaerobic chamber and serial dilutions of the culture samples were made in liquid CP medium (60). Dilutions were plated on CP plates and incubated in custom-built anaerobic jars with Gas-Pak envelopes (Beckton Dickinson, Cockeysville, Maryland), catalyst (Beckton Dickinson), and a sulfide generating system (Wahlund and Madigan 1995) for 5–7 days at 48°C at which time colonies were counted.

Sulfur compound assays

Sulfide was quantitated by the methylene blue assay (Trüper and Schlegel 1964). Thiosulfate was measured after conversion to Fe–SCN complex in the presence of Cu^{2+} ions as described by Westley (1987).

Subcellular fractionation of C. tepidum

Autotrophic cultures (100 ml per culture) of *C. tepidum* strains WT2321 and $\Omega::RLP$ were grown to mid-exponential phase ($\sim 80\text{--}100 \mu\text{g protein ml}^{-1}$). Cells were collected by centrifugation at $7500 \times g$ for 5 min at room temperature. Secreted proteins were recovered by recentrifuging spent medium prior to concentration from 100 ml to $\sim 150 \mu\text{l}$ through a Centricon-15 concentrator with a 5 kDa molecular weight cutoff filter. Periplasm-enriched fractions were prepared by mild osmotic shock in the absence of lysozyme, as originally described for *Alcaligenes faecalis* (Zhu et al. 1999). Cells recovered from the osmotic shock were resuspended in cold lysis buffer and treated as above to produce the soluble fraction. The pellet resulting from centrifugation at $150,000 \times g$ was washed once by resuspension in cold lysis buffer followed by a 30 min centrifugation at $150,000 \times g$. The resulting pellet constituted the membrane fraction and was resuspended in cold lysis buffer + 1% SDS. Extracts prepared by this method were normalized for gel loading by their absorbance at 280 nm because they could not be reproducibly quantitated using either Lowry or Bradford colorimetric assays.

Results and discussion

General comparison of soluble proteins from strain WT2321 and $\Omega::RLP$

Examples of gels used to compare the proteomes of strain WT2321 and strain $\Omega::RLP$ are shown (Figure 2). Comparison across three independent cultures for each strain led to the identification of a set of 350 individual soluble polypeptides that could be matched across all gels and compared quantitatively. Based on the prediction of 2228 ORFs in the total *C. tepidum* genome (Eisen et al. 2002), this means that approximately 16% of the potential proteome was observed in this comparison of soluble proteins, assuming that each visualized polypeptide corresponds to one protein. This is not a valid assumption for all proteins (see Figures 3 and 4) and a more accurate estimate is probably between 10% and 15% of the total proteome. The results of that comparison (Table 2) indicated that approximately 13% of the *C. tepidum* proteome, or one out of every eight polypeptides observed on a two-dimensional gel, significantly changed in abundance due to the loss

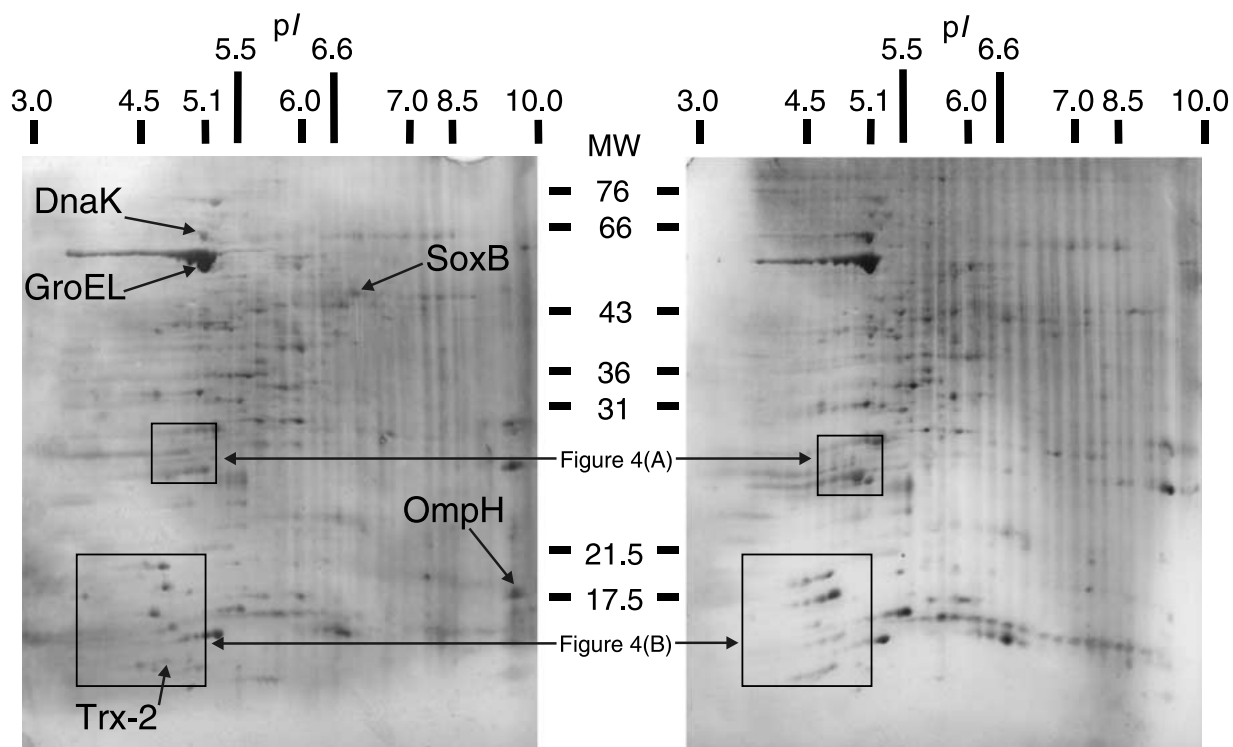


Figure 2. Two-dimensional SDS-PAGE separations of soluble extracts from strain WT2321 (A) and strain Ω ::RLP (B). First dimension separation was performed in a pH 3–10 gradient and second dimension separation utilized an 8–16% acrylamide gradient gel. Standards for pI and MW were from independently run gels of 2D SDS-PAGE standards (Bio-Rad). Identities of proteins were determined by MALDI-TOF MS as described in Materials and methods. Boxed regions containing proteins with expression or migration differences are expanded in Figure 4.

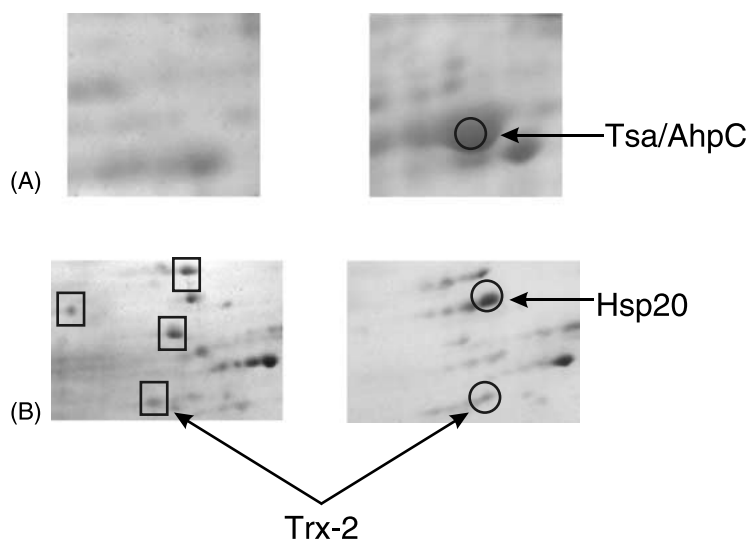


Figure 3. Expanded view of regions indicated in Figure 2. Left hand panels are of strain WT2321 extract and right hand panels are of strain Ω ::RLP extract. (A) Region containing the Tsa/AhpC homolog previously identified as a hyper-expressed protein in strain Ω ::RLP. (B) Region containing a number of polypeptides with higher abundance in strain WT2321 (squares) or strain Ω ::RLP (circles). Protein identities were determined by MALDI-TOF MS or by LC-MS/MS (Table 4).

of the RLP. Similar numbers of polypeptides were seen to increase or decrease in abundance in strain Ω ::RLP.

One goal of this study was to identify protein markers that could be used as landmarks for future studies. Several abundant polypeptides from widely separated

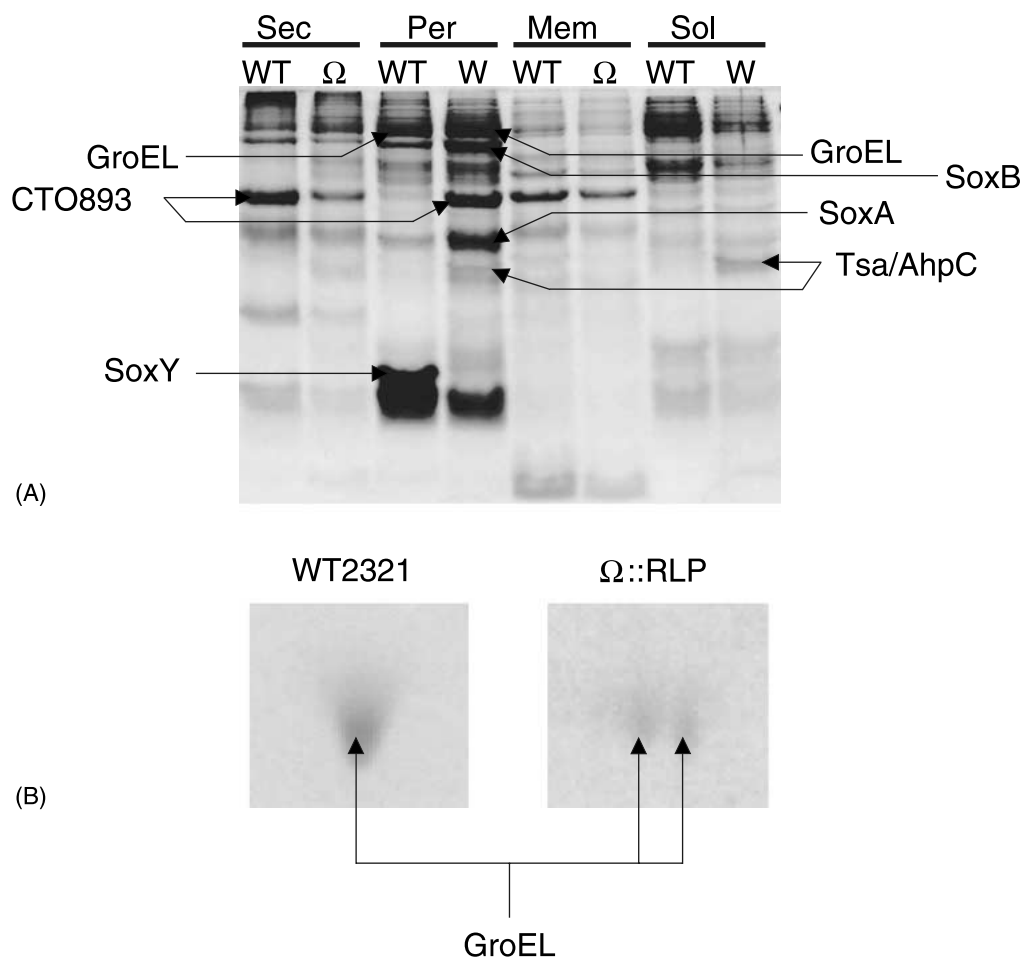


Figure 4. Comparison of subcellular fractions of strain WT2321 and strain $\Omega::\text{RLP}$. (A) SDS-PAGE of secreted (Sec), periplasm-enriched (Per), membrane (Mem) and soluble (Sol) fractions in a 15% acrylamide gel. Indicated proteins were identified by MALDI-TOF MS or LC-MS/MS (Table 5). (B) Close-up of 2D SDS-PAGE separation of periplasm-enriched extracts from strain WT2321 and strain $\Omega::\text{RLP}$ demonstrating twinning of GroEL in strain $\Omega::\text{RLP}$. Each polypeptide was identified as GroEL by MALDI-TOF MS (Table 5).

Table 2. Summary of 2D SDS-PAGE comparison of soluble proteins from *C. tepidum* strain WT2321 and $\Omega::\text{RLP}$

Total matched proteins	350	
Proteins > 3X over-expressed in $\Omega::\text{RLP}$	24	Max. 18.1X Avg. 5.7X
Proteins > 3X under-expressed in $\Omega::\text{RLP}$	21	Max. 40.1X Avg. 6.1X
Total number of proteins changed >3X in $\Omega::\text{RLP}$	45 (12.9%)	

Table 3. Comparison of predicted and observed pI and MW for *C. tepidum* landmark proteins indicated in Figure 2

Protein	Gene	Predicted pI/MW ^a	Observed pI/MW ^b
DnaK	<i>CT0643</i>	5.2/68.5	5.1/65
GroEL	<i>CT0530</i>	5.2/58.1	5.1/60
SoxB	<i>CT1970</i>	7.0/68.4 (6.6/63.6)	6.1/46
OmpH	<i>CT0254</i>	9.5/20.4	9.5/18
Trx-2	<i>CT1970</i>	4.9/11.9	4.7/12

^a Calculated using pI/MW tool at the ExPASy Molecular Biology Server (www.expasy.ch) using sequences from the *C. tepidum* annotation at The Institute for Genomic Research website (www.tigr.org).

^b Derived by comparison to 2D SDS-PAGE standards separated under the same conditions in independent gels.

areas of the gels were identified (Figure 3) and the observed pI/MW values derived from separately run standard gels compared to predicted pI/MW values derived from the predicted ORFs

encoding the proteins. Good agreement was found in most cases except for the SoxB protein (Table 3).

Table 4. Proteins showing altered abundance or migration in soluble extracts of strain Ω ::RLP compared to strain WT2321 (Figure 2)

Protein	Gene	Fold difference Ω ::RLP/WT2321	ID method	Z-score ^a	% Coverage ^b
Tsa/AhpC	<i>CT1492</i>	10.5	MALDI	1.78	46
				<i>E</i> -value ^c	Number of peptides ^d
Hsp20	<i>CT1970</i>	3.0	LC-MS/MS	6.3×10^{-14}	8
Trx-2	<i>CT0841</i>	Basic pI shift in Ω ::RLP	LC-MS/MS	7.7×10^{-7}	3

^a Confidence score as reported by Mascot ProFound search engine. In all cases, *C. tepidum* sequences were the best scoring match.

^b Percent of amino acid sequence of the sequence match that corresponded to peptide masses in the MALDI-TOF peak list.

^c Confidence score as reported by Sonar MS/MS search engine. Similar to BLAST *E*-values, it indicates the probability that the matches found are random based on the size of the database searched, in this case the NCBI non-redundant database. In all cases, the indicated *C. tepidum* sequences were the best match.

^d Number of individual peptides from LC-MS/MS data displaying a match to the proposed sequence match.

The *C. tepidum* SoxB protein, a subunit of the predicted thiosulfate oxidizing complex (Wodara et al. 1994; Friedrich et al. 2001), consistently migrated at ~46 kDa, faster than the observed mass for GroEL, at ~60 kDa. The predicted SoxB protein, at 68 kDa, is approximately 10 kDa larger than the predicted GroEL protein at 59.8 kDa. Part of this discrepancy lies in the fact that SoxB is a periplasmic enzyme and the annotated ORF contains a signal sequence. Another part of the discrepancy is that the SoxB ORF likely was assigned the wrong start site, including 32 additional codons that are not supported by BLASTP alignments against the characterized *Paracoccus pantotrophus* SoxB protein. The *P. pantotrophus* SoxB protein has a predicted mass of 58.8 kDa that is closely matched by its observed mass of 59 kDa in SDS-PAGE (Friedrich et al. 2000). However, the considerations above predicted a molecular mass of 64 kDa for the *C. tepidum* Sox B protein, which is still significantly higher than the observed molecular mass of 48 kDa.

Identification of specific proteins with differential abundance in strain WT2321 and Ω ::RLP

We previously showed that *C. tepidum* strain Ω ::RLP constitutively over-produces two oxidative stress response proteins, Tsa/AhpC (CT1492) and Fe-SOD (CT1211) homologs, that co-migrate on SDS-PAGE gels. However, previous experiments failed to determine the separate contribution of each protein (Hanson and Tabita 2001). In the current study, it is now established that the Tsa/AhpC protein encoded by gene

CT1492 is the most abundant hyper-accumulated protein in strain Ω ::RLP (Figure 3, Table 4). An additional hyper-expressed protein was identified in strain Ω ::RLP as a putative Hsp20 chaperonin encoded by gene *CT1970*.

The Hsp20 family is a large group of related proteins with an average molecular mass of 20 kDa. They are found in bacteria, archaea, eukaryotes and include the recently crystallized MJ0285 protein from *Methanococcus jannaschii* (Kim et al. 1998) as well as α -crystallin A and B chains of vertebrates (de Jong et al. 1993). Members of this family that have been functionally characterized tend to be synthesized at higher levels during heat and other stresses; they are highly oligomeric and apparently serve to prevent denaturation and/or aggregation of unfolded proteins by direct binding (Saibil 2000). This protein family has greatly expanded in plants resulting in four distinct classes with distinct subcellular localization and regulation (Waters 1995). Expression of Hsp20 family members in *Escherichia coli* can induce increased resistance to thermal stress (Soto et al. 1999) as can overexpression in the cognate host (Sun et al. 2001). The hyper-accumulation of an Hsp20 family chaperonin in *C. tepidum* may suggest that strain Ω ::RLP experiences unfolded protein stress or that chaperonins are part of an oxidative stress regulon that is activated in strain Ω ::RLP. An additional indication of such a response in strain Ω ::RLP to unfolded protein or oxidative stress was the observation of a modified form of GroEL, discussed below.

In addition to proteins showing a greater than 3-fold change in abundance, proteins displaying multiple isoforms were identified. An example is a thioredoxin, Trx-2, encoded by gene *CT0841*. Both isoforms appeared to be present in strain Ω ::RLP and strain WT2321 and they differed in their isoelectric point (pI). The more positive pI isoform was approximately 2- to 3-fold more abundant in strain Ω ::RLP compared to strain WT2321 (circle in right panel of Figure 3A) and vice versa for the more acidic isoform (square in left panel of Figure 5A). Shifts in isoelectric point can result from post-translational modification.

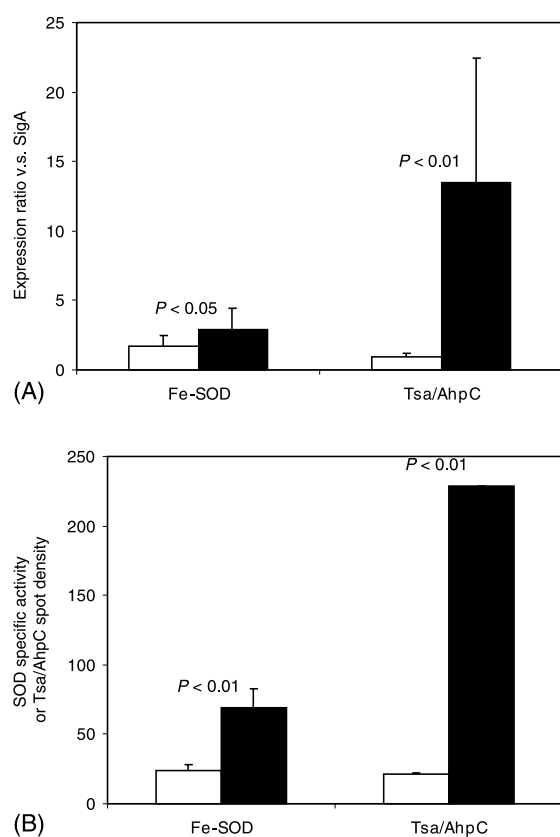


Figure 5. Increased transcription of genes encoding the *C. tepidum* Fe-SOD and Tsa/Ahp homologs accounts for the observed increases in SOD activity and Tsa/AhpC protein levels. (A) Expression ratios of each transcript relative to transcripts encoding SigA in strain WT2321 (white bars) and strain Ω ::RLP (black bars). (B) Comparison of SOD activity or Tsa/AhpC protein levels in strain WT2321 (white bars) and strain Ω ::RLP (black bars). The vertical axis units are specific activity [Units (mg protein)⁻¹] for the SOD data and spot density ($\times 10^2$ ppm, see 'Materials and methods' for unit explanation) for the Tsa/AhpC data. The data are the mean of three independent cultures for each measurement with the error bars representing the standard deviation about the mean. *P*-values resulting from *t*-tests on each comparison are noted above the data.

A recent study indicated that human thioredoxin is glutathionylated in response to oxidative stress *in vivo* (Casagrande et al. 2002) and suggests that thioredoxin modification may have regulatory significance. The nature and significance of this potential modification of Trx-2 from *C. tepidum* is unclear at this time.

Elevated transcription causes oxidative stress protein over-abundance in C. tepidum strain Ω ::RLP

The most logical explanation for the observed hyper-accumulation of the *C. tepidum* Tsa/AhpC and Fe-SOD protein homologs is increased transcription of their cognate genes. Transcript levels were determined for the genes encoding Tsa/AhpC (*CT1492*) and Fe-SOD (*CT1211*) homologs as well as the gene encoding the major housekeeping RNA polymerase sigma factor, SigA (*CT1551*) (Gruber and Bryant 1998; Eisen et al. 2002). Transcript levels in strains WT2321 and Ω ::RLP were determined using a quantitative RT-PCR assay. Amplicons for quantitation of each gene's mRNA are described in 'Materials and methods'. Melt curve determinations for each amplicon gave a single peak and agarose gel electrophoresis of the products from genomic DNA controls or reverse transcription reaction products confirmed that each primer pair produced a single, identical product regardless of the template (data not shown). The gene encoding the major sigma factor SigA served as an internal standard for normalization in this experiment and controlled for any effects due to variations in RNA preparation, reverse transcription efficiency or amplification. Based on the observation that approximately 80–85% of the proteins matched between strains WT2321 and Ω ::RLP were present at similar levels (Table 2), it was expected that the level of SigA protein and transcript levels would be essentially the same in the two strains. Simple division of the transcript-specific copy numbers, determined in the quantitative PCR reactions, gave an expression ratio of the Tsa/AhpC or Fe-SOD transcripts relative to SigA. This ratio was then used to compare expression of the homolog genes between strains WT2321 and Ω ::RLP.

The quantitative PCR data indicated that there was a 14.2-fold increase in transcript levels for the gene encoding the Tsa/AhpC homolog in strain Ω ::RLP compared to strain WT2321 (Figure 5A). The gene encoding the Fe-SOD homolog appeared to be transcribed at a 1.7-fold higher level in strain Ω ::RLP compared to strain WT2321. Densitometry of the

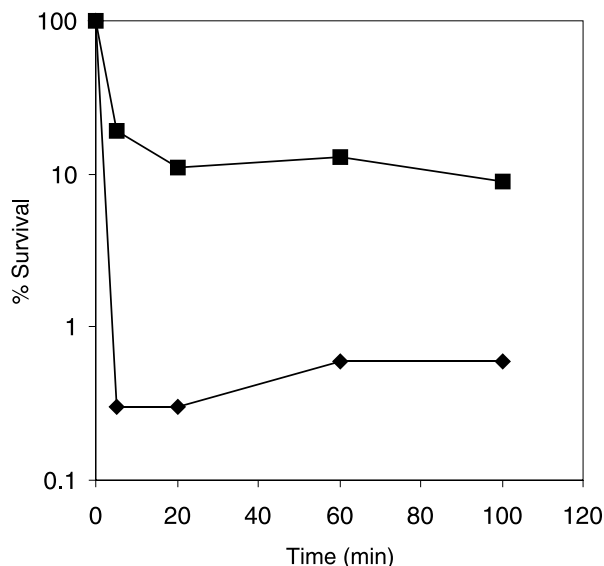


Figure 6. *C. tepidum* strain $\Omega::RLP$ (■) is more resistant to H_2O_2 exposure than strain WT2321 (◆). Viability was determined using a plate count assay over time in cultures that were amended to $400 \mu M$ H_2O_2 immediately after the zero time point was taken. The data are presented as the percentage of colony forming units at time zero remaining at each time point.

Tsa/AhpC homolog protein indicated that it was present at a 10.5-fold higher level in strain $\Omega::RLP$ compared to strain WT2321 (Figure 5A). SOD activity was elevated 3-fold in strain $\Omega::RLP$ compared to strain WT2321 [Figure 5A, also see (Hanson and Tabita 2001)]. *T*-tests of each data set indicated that the observed differences were statistically significant. The close agreement between these independent measures of gene expression and protein accumulation/activity for both the Tsa/AhpC and Fe-SOD homologs indicated that elevated transcription accounted for the observed over-abundance of these two proteins in strain $\Omega::RLP$. This data also clearly demonstrated that strain $\Omega::RLP$ over-produced higher levels of the Tsa/AhpC homolog compared to the Fe-SOD homolog. This result could imply that over-expression of the gene encoding the Tsa/AhpC homolog, *CT1492*, is more important to strain $\Omega::RLP$ or is more responsive to a signal that is generated in the $\Omega::RLP$ background.

C. tepidum strain $\Omega::RLP$ is more resistant to oxidative stress than strain WT2321

An initial assessment of the functionality of the various identified stress proteins was made by comparing the resistance of *C. tepidum* strain $\Omega::RLP$ and wild-type strain WT2321 to H_2O_2 exposure by measuring

viable cell populations in stressed cultures. A level of $400 \mu M$ H_2O_2 was used for the challenge. This level of H_2O_2 is significantly lower than conditions used to oxidatively stress other organisms (Mongkolsuk et al. 1998; Takemoto et al. 1998; King et al. 2000; Yamamoto et al. 2000; Rince et al. 2001). Following only 10 min of H_2O_2 exposure, cultures of strain $\Omega::RLP$ contained approximately 10-fold higher levels of viable cells than cultures of strain WT2321 (Figure 6). This result strongly implicated the identified oxidative stress proteins in active resistance to oxidative stress, implying that the proteins were not quiescent or synthesized in inactive forms in the absence of stress. Genetic experiments are currently underway to further probe the contribution of the genes encoding the Tsa/AhpC and Fe-SOD to the observed increase in oxidative stress resistance in strain $\Omega::RLP$.

Strain Ω::RLP is defective for thiosulfate, but not sulfide, consumption

Strain $\Omega::RLP$ was previously shown to accumulate higher levels of elemental sulfur compared to strain WT2321, the wild type parent (Hanson and Tabita 2001). Oxidation of sulfide and thiosulfate was examined in both strains to determine if the defect was specific to elemental sulfur utilization or if it affected the ability to utilize all reduced sulfur compounds. The levels of sulfide and thiosulfate in batch autotrophic cultures of strains $\Omega::RLP$ and WT2321 were measured over time (Figure 7). Cultures of strain $\Omega::RLP$ consumed sulfide at the same rate as wild type (Figure 7A). Sulfide is most likely oxidized via a sulfide quinone oxidoreductase in *C. tepidum* (Shahak et al. 1992; Eisen et al. 2002; Verte et al. 2002). Clearly, this system appeared to be unaffected by the loss of the RLP.

Thiosulfate was not consumed to any significant extent by strain $\Omega::RLP$ during the course of the experiment (Figure 7B). Strain WT2321, in contrast, oxidized most of the thiosulfate provided in the medium. This result suggested that the defect in strain $\Omega::RLP$ affected both elemental sulfur and thiosulfate oxidation, which may indicate that oxidation of both compounds relies on a common pathway at some point during their metabolism by *C. tepidum*.

SoxY protein abundance is altered in strain Ω::RLP compared to strain WT2321

Given that strain $\Omega::RLP$ displays a thiosulfate oxidation defect, we attempted to ascertain whether

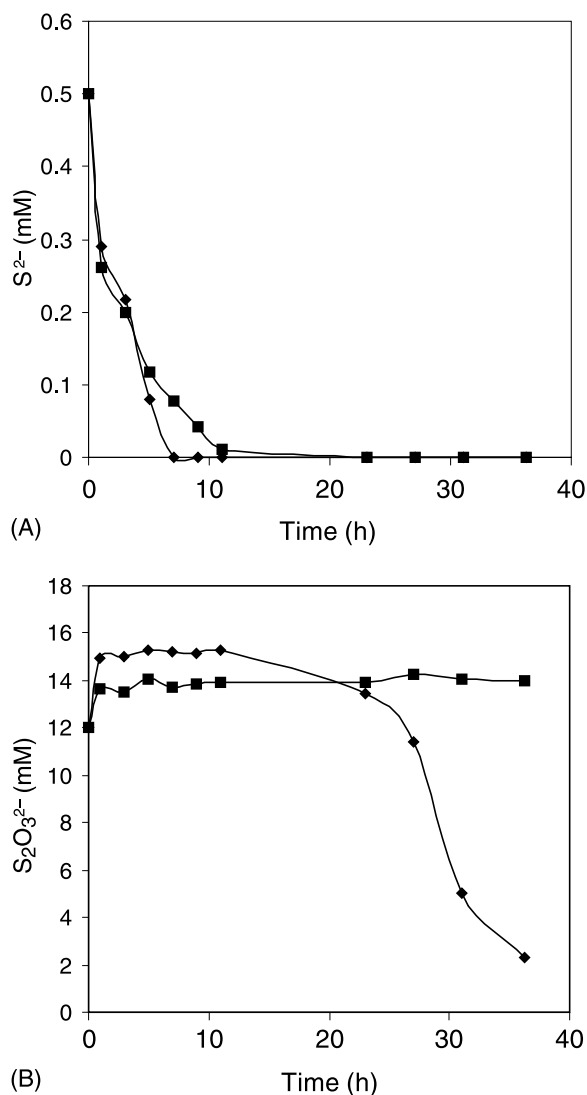


Figure 7. Concentration of reduced sulfur compounds in batch cultures of strain WT2321 (diamonds) or strain $\Omega::RLP$ (squares) during growth. (A) Sulfide concentration determined using methylene blue assay. (B) Thiosulfate concentration determined after conversion to thiocyanate.

the Sox proteins were present in the periplasm of strain $\Omega::RLP$. This would discriminate between strain $\Omega::RLP$ being unable to produce Sox proteins due to gene expression defects as opposed to defects preventing the catalysis of existing Sox complexes. The *C. tepidum* genome contains an operon that encodes a homolog of the well-studied periplasmic sulfur oxidizing (Sox) system of *P. pantotrophus* GB17 which encodes thiosulfate:cytochrome *c* oxidoreductase. A recent review describes the components of the sys-

tem, their functions and the distribution of *sox* genes among various bacteria (Friedrich et al. 2001). The *C. tepidum* operon lacks various genes, including those encoding the SoxCD component. SoxCD is a periplasmic molybdenum-containing sulfur dehydrogenase that is required for the full oxidation of thiosulfate *in vitro* (Rother et al. 2001). The substrate of SoxCD is a protein bound cysteine-S-sulfide (S-thiocysteine) bound on SoxY in the SoxYZ subunit of the Sox complex (Friedrich et al. 2001; Quentmeier and Friedrich 2001; Rother et al. 2001). The products of the reaction are sulfate and the regenerated cysteine in SoxY.

Published protocols for producing periplasmic fractions from various organisms resulted in lysis of *C. tepidum* as judged by the release of Bchl *c*, which normally resides in the interior of the cell in the chlorosomes (Vassilieva et al. 2002). Absorbance spectra of the fractions produced by a gentle osmotic shock in the absence of lysozyme indicated that more than 95% of the Bchl *c* was retained in the membrane fraction with very low levels of Bchl *c* contamination in the secreted, periplasmic or soluble fractions (data not shown). SDS-PAGE comparisons of these fractions also indicated that unique proteins were present in each fraction (Figure 4). However, immunoblot analysis of the fractions revealed that the periplasmic fraction was contaminated by ATP-citrate lyase and RLP, both of which were expected to be cytoplasmic (data not shown). Identification of prominent polypeptides in the osmotic shock fraction indicated that it did indeed contain predicted periplasmic proteins; SoxA and SoxB were identified in strain $\Omega::RLP$ and SoxY was identified in strain WT2321 (Figure 4A, Table 5). This result indicated that at least some of the Sox proteins were produced in strain $\Omega::RLP$ and eliminated a complete lack of Sox gene expression as the cause of the thiosulfate oxidation defect in strain $\Omega::RLP$. However, proteins corresponding to the *Tsa/AhpC* homolog as well as GroEL were also detected in periplasm-enriched samples (see below). Neither protein should be periplasmically localized, which further indicated that the osmotic shock produced only a periplasm-enriched fraction.

Comparison of periplasm-enriched fractions immediately revealed that a ~ 17 kDa polypeptide present at high levels in strain WT2321 was not detectable in strain $\Omega::RLP$ (Figure 4A). This polypeptide was identified as SoxY (Table 5). SoxY is the carrier protein of the Sox complex, and binds thiosulfate through

Table 5. Identification of proteins from secreted and periplasm-enriched fractions (Figure 4) of strain Ω ::RLP and strain WT2321

Protein	Gene	Strain	Fraction	ID Method	Z-score	% coverage
Conserved hypothetical	<i>CT0893</i>	WT2321	Secreted	MALDI	1.73	40
Conserved hypothetical	<i>CT0893</i>	Ω ::RLP	P-enriched ^a	MALDI	1.65	45
Tsa/AhpC	<i>CT1492</i>	Ω ::RLP	P-enriched	MALDI	1.78	46
SoxB	<i>CT1021</i>	Ω ::RLP	P-enriched	MALDI	2.39	31
SoxA	<i>CT1019</i>	Ω ::RLP	P-enriched	MALDI	2.11	42
GroEL	<i>CT0530</i>	WT2321	P-enriched	MALDI	2.34	41
GroEL-negative isoform	<i>CT0530</i>	Ω ::RLP	P-enriched	MALDI	2.34	37
GroEL-positive isoform	<i>CT0530</i>	Ω ::RLP	P-enriched	MALDI	2.34	41
					<i>E</i> -value	Number of peptides
SoxY	<i>CT1017</i>	WT2321	P-enriched	LC-MS/MS	1.8×10^{-2}	1

^a Periplasm-enriched fraction.

the sulfidic end of the molecule by a cysteine-S-sulfide bond (Quentmeier and Friedrich 2001). This observation suggests that the thiosulfate oxidation defect resulted from drastically decreased abundance of SoxY in strain Ω ::RLP. However, the proximal cause for decreased abundance of SoxY protein in strain Ω ::RLP is not clear. It is possible that the gene encoding SoxY may not be expressed in strain Ω ::RLP, but such a mechanism would likely be complicated. SoxY is the third gene in a thirteen gene operon (*CT1015-CT1027*) encoding the Sox complex (Eisen et al. 2002; Verte et al. 2002). This cluster includes the genes encoding SoxB and SoxA, which are located transcriptionally downstream of the gene encoding SoxY. Thus, if the gene encoding SoxY was not expressed, we would not expect that the genes encoding SoxA and SoxB would be expressed either. Our results indicated that both SoxA and SoxB were synthesized in strain Ω ::RLP, indicating that multiple transcripts, differential stability or degradation of mRNA or protein are necessary to explain the lowered abundance of SoxY in *C. tepidum*.

The elemental sulfur oxidation and growth phenotypes of strain Ω ::RLP can be rescued with 0.5 mM cysteine, suggesting that the defect may lie in low molecular weight thiol metabolism (Hanson and Tabita 2001). We do not have conclusive data at this time for the effect of low molecular weight thiols on the thiosulfate oxidation defect in strain Ω ::RLP. Low molecular weight thiols have been postulated to be involved in elemental sulfur oxidation in phototrophic bacteria (Brune 1989, 1995). Specifically, glutathione amide appears to cycle between thiol and perthiol

forms when *A. vinosum* oxidizes stored elemental sulfur globules (Bartsch et al. 1996). *C. limicola* and *C. tepidum* appear to contain structurally novel low molecular weight thiols (Fahey et al. 1987; Hanson and Tabita, unpublished). Thus, there is a distinct possibility that RLP is involved in synthesizing or cycling these low molecular weight thiol compounds during sulfur compound oxidation.

Furthermore, the *C. tepidum* genome does not encode a complete system for the oxidation of thiosulfate. *C. tepidum* specifically lacks genes encoding SoxCD which acts as a sulfur dehydrogenase on a SoxY bound sulfur atom (Quentmeier and Friedrich 2001). This suggests that *C. tepidum* possesses an alternative mechanism for oxidation of SoxY bound sulfur. We speculate that this mechanism is transfer of the SoxY bound sulfur atom to a low molecular weight thiol acceptor. The product of this transfer would be a low molecular weight perthiol, which is structurally analogous to heterodisulfides produced during methanogenesis and archaeal C1 metabolism (Setzke et al. 1994; Ide et al. 1999). The *C. tepidum* genome encodes a homolog of an archaeal heterodisulfide oxidoreductase with the closest functionally characterized homolog being that of *Methanosarcina mazei* Gö1 (Ide et al. 1999; Eisen et al. 2002). These genes are localized in the *C. tepidum* genome along with genes encoding a copy of the *A. vinosum dsr* system, previously implicated in elemental sulfur oxidation (Pott and Dahl 1998). This potential sulfur oxidation island also includes genes encoding ATP-sulfurylase and APS reductase. The presence of these

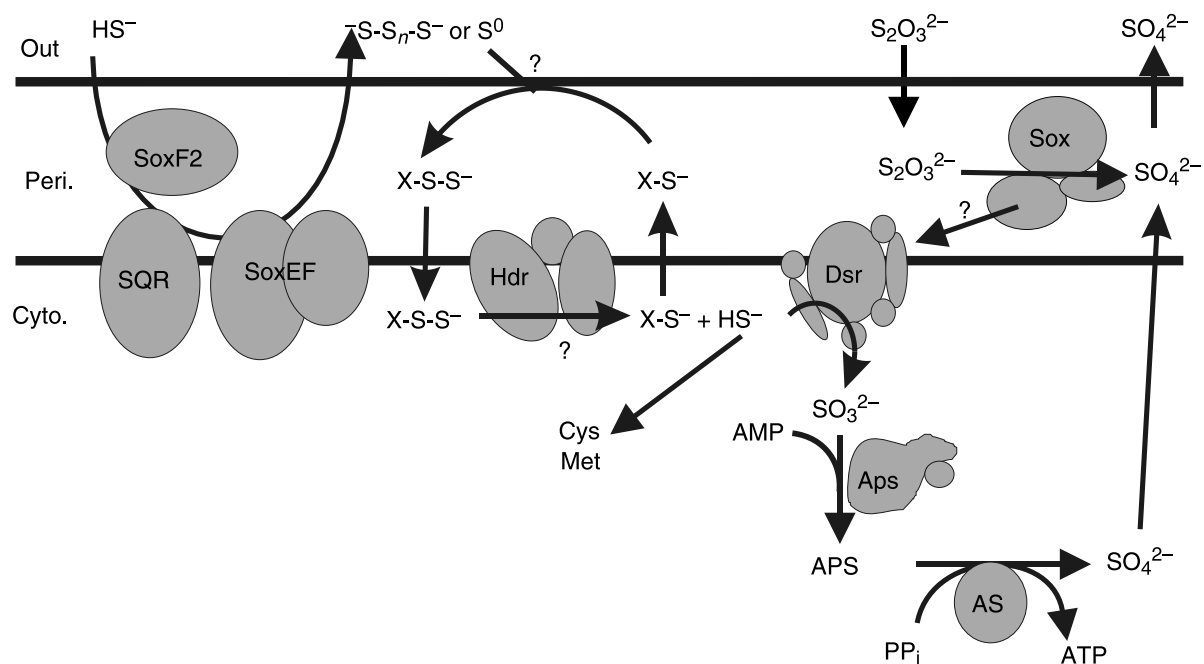


Figure 8. Proposed oxidative sulfur metabolism scheme in *C. tepidum*. A similar pathway was proposed in the published analysis of the *C. tepidum* genome sequence (Eisen et al. 2002). Areas of doubt requiring further experimental confirmation are indicated by question marks. Abbreviations: HS^- , sulfide; $^-S-S_n-S^-$, polysulfide; S^0 , elemental sulfur; $\text{S}_2\text{O}_3^{2-}$, thiosulfate, SO_3^{2-} , sulfite; SO_4^{2-} , sulfate; X-S^- , low molecular weight thiol; SQR, sulfide quinone oxidoreductase; Sox, thiosulfate oxidation complex; Hdr, possible heterodisulfide reductase; Dsr, dissimilatory sulfite reductase homologs; Aps, adenosine phosphosulfate reductase; AS, ATP-sulfurylase. The genes encoding the Hdr, Dsr, Aps and AS components are co-localized on the *C. tepidum* genome in a potential sulfur metabolism island containing ~28 genes encoding these functions and conserved hypothetical proteins (*CT0841-CT0868*) (Eisen et al. 2002).

genes leads to a proposed pathway for the oxidation of elemental sulfur globules and the S-thiocysteine of SoxY via a low molecular weight thiol intermediate through sulfite and APS, leading to sulfate (Figure 8). An attractive feature of this model is the conservation of one molecule of ATP by reversal of the ATP sulfurylase reaction.

As shown in the model, elemental sulfur is deposited extracellularly in *C. tepidum* and other green sulfur bacteria (Wahlund et al. 1991). Extracellular elemental sulfur can be oxidized by green sulfur bacteria (Paschinger et al. 1974) in a light dependent process, but thus far no specific proteins involved in this process have been identified. Current models of sulfur oxidation in *C. tepidum* do not account for the extracellular localization of elemental sulfur (Eisen et al. 2002), but it is known that strain $\Omega::\text{RLP}$ displays a defect in elemental sulfur metabolism (Hanson and Tabita 2001). A 35 kDa polypeptide was retained in the periplasm-enriched fraction of strain $\Omega::\text{RLP}$, but co-migrated with a polypeptide in the secreted fraction of strain WT2321 (Figure 4A). Both polypeptides were identified as a conserved hypothetical

protein, encoded by *CT0893*. No significant structural or sequence motifs were found in this protein that might shed light on its physiological role. However, its apparent secretion by strain WT2321 and lack of secretion by strain $\Omega::\text{RLP}$ make it a candidate protein for extracellular elemental sulfur oxidation. Further genetic experiments will be undertaken to test this hypothesis.

Potential modification of GroEL in strain $\Omega::\text{RLP}$

2D SDS-PAGE separations of periplasmic fractions from strain $\Omega::\text{RLP}$ and WT2321 revealed a protein that was consistently twinned in extracts from strain $\Omega::\text{RLP}$ (Figure 4B) suggesting posttranslational modification resulting in isoforms. All three proteins were identified as GroEL, encoded by gene *CT0530* (Table 5). This discovery was serendipitous in that the subtle shift was not observed in soluble extracts due to the abundance of the GroEL protein (Figure 2). The osmotic shock employed to produce the periplasm-enriched fraction apparently also released a portion of some of the most abundant proteins

in the cytoplasm, uncovering this potentially modified population of GroEL molecules.

The nature of the apparent modification of GroEL has not been elucidated. However, the more negative GroEL isoform observed in strain Ω ::RLP had lower sequence coverage than the other isoform (Table 5). This corresponded to a larger number of unmatched masses present in the MALDI peak list. These masses could not be attributed to background peaks arising from trypsin, MALDI matrix, or acrylamide adducts (data not shown). Searches of these unmatched masses against *C. tepidum* GroEL for common modifications such as phosphorylation, methylation, acetylation, biotinylation, and others including side chain oxidation and degradation, failed to identify the potential modification of GroEL in strain Ω ::RLP. Further LC-MS/MS experiments should determine whether the more negatively charged GroEL isoform observed in strain Ω ::RLP is the result of a physiologically significant modification. Modification of GroEL is not unprecedented; phosphorylated GroEL was found in heat stressed *E. coli* (Sherman and Goldberg 1992). Phosphorylation allowed GroEL to release from unfolded protein substrates in the absence of GroES and was proposed to enhance the function of GroEL in stressed cells. Similarly, the human GroEL homolog, Hsp60, was also recently found as a glutathionylated form during oxidative stress (Fratelli et al. 2002) and appears to be synthesized at elevated rates following exposure to peroxide stress (Mitsumoto et al. 2002).

Conclusions

The *C. tepidum* and *C. limicola* RLP sequences form part of a distinct cluster within the larger group of all known RLP molecules; this cluster includes RLP's from *R. palustris* and *A. vinosum* (Figure 1). Indeed, there appear to be at least two, and possibly three subclasses of RLP, which will undoubtedly become clearer as more genomic sequences become completed. *C. tepidum*, *C. limicola*, *R. palustris* and *A. vinosum* are phototrophic sulfur oxidizers. Given that the *C. tepidum* RLP appears to affect both elemental sulfur and thiosulfate oxidation, we speculate that the RLP's in these organisms may perform similar functions. The results presented in this study, along with earlier data, clearly indicate that the *C. tepidum* RLP plays a distinct physiological role from that proposed for the *yrkW*-encoded RLP gene product of *B. subtilis*. Further studies of close relatives to the

C. tepidum protein should clarify this point. While no concrete biochemical activity is currently known to be catalyzed by *C. tepidum* RLP, we have made progress in further defining the phenotype of strain Ω ::RLP. This, we feel, is an important approach towards unlocking this puzzle. Additionally, several loci for future genetic and biochemical analyses related to sulfur metabolism, the noted oxidative stress response, and the integration of both processes in *C. tepidum* metabolism have been identified.

Acknowledgements

Preliminary *C. tepidum* sequence data was obtained from The Institute for Genomic Research website at <http://www.tigr.org>. The authors thank Mike Zianni of the Plant Microbe Genomics Facility for assistance with quantitative PCR determinations and Kari Green-Church and Nan Kleinholz of The Campus Chemical Instrument Center for MS protein identification. This project was supported in part by Department of Energy grant DE-FG02-91-ER20033 and by Public Health Services grant GM24497 from the National Institutes of Health.

References

- Ausubel FM, Brent R, Kingston RE, Moore DD, Seidman JG, Smith JA and Struhl K (1987) Current Protocols In Molecular Biology. Green Publishing Associates/Wiley Interscience, New York
- Bartsch R, Newton G, Sherril C and Fahey R (1996) Glutathione amide and its perthiol in anaerobic sulfur bacteria. *J Bacteriol* 178: 4742–4746
- Brune D (1989) Sulfur oxidation by phototrophic bacteria. *Biochim Biophys Acta* 975: 189–221
- Brune DC (1995) Sulfur compounds as photosynthetic electron donors. In: Blankenship RE, Madigan MT and Bauer CE (eds) Anoxygenic Photosynthetic Bacteria, pp 847–870. Kluwer Academic Publishers, Dordrecht, The Netherlands
- Casagrande S, Bonetto V, Fratelli M, Gianazza E, Eberini I, Massignan T, Salmona M, Chang G, Holmgren A and Ghezzi P (2002) Glutathionylation of human thioredoxin: a possible crosstalk between the glutathione and thioredoxin systems. *Proc Natl Acad Sci USA* 99: 9745–9749
- de Jong WW, Leunissen JA and Voorter CE (1993) Evolution of the alpha-crystallin/small heat-shock protein family. *Mol Biol Evol* 10: 103–126
- Eisen JA, Nelson KE, Paulsen IT, Heidelberg JF, Wu M, Dodson RJ, Deboy R, Gwinn ML, Nelson WC, Haft DH, Hickey EK, Peterson JD, Durkin AS, Kolonay JL, Yang F, Holt I, Umayam LA, Mason T, Brenner M, Shea TP, Parksey D, Nierman WC, Feldblyum TV, Hansen CL, Craven MB, Radune D, Vemathavan J, Khouri H, White O, Gruber TM, Ketchum K, Venter JC, Tettelin H, Bryant D and Fraser CM (2002) The complete genome sequence of *Chlorobium tepidum* TLS, a photosynthetic,

- anaerobic, green-sulfur bacterium. *Proc Natl Acad Sci USA* 99: 9509–9514
- Ellis R (1979) The most abundant protein in the world. *Trends Biochem Sci* 4: 241–244
- Ezaki S, Maeda N, Kishimoto T, Atomi H and Imanaka T (1999) Presence of a structurally novel type ribulose-bisphosphate carboxylase/oxygenase in the hyperthermophilic archaeon, *Pyrococcus kodakaraensis* KOD1. *J Biol Chem* 274: 5078–5082
- Fahey RC, Buschbacher RM and Newton GL (1987) The evolution of glutathione metabolism in phototrophic microorganisms. *J Mol Evol* 25: 81–88
- Fratelli M, Demol H, Puype M, Casagrande S, Eberini I, Salmona M, Bonetto V, Mengozzi M, Duffieux F and Miclet E et al. (2002) Identification by redox proteomics of glutathionylated proteins in oxidatively stressed human T lymphocytes. *Proc Natl Acad Sci USA* 99: 3505–3510
- Friedrich CG, Quentmeier A, Bardischewsky F, Rother D, Kraft R, Kostka S and Prinz H (2000) Novel genes coding for lithotrophic sulfur oxidation of *Paracoccus pantotrophus* GB17. *J Bacteriol* 182: 4677–4687
- Friedrich CG, Rother D, Bardischewsky F, Quentmeier A and Fischer J (2001) Oxidation of reduced inorganic sulfur compounds by bacteria: emergence of a common mechanism? *Appl Environ Microbiol* 67: 2873–2882
- Gruber TM and Bryant DA (1998) Characterization of the group 1 and group 2 sigma factors of the green sulfur bacterium *Chlorobium tepidum* and the green non-sulfur bacterium *Chloroflexus aurantiacus*. *Arch Microbiol* 170: 285–296
- Grundy FJ and Henkin TM (1998) The S box regulon: a new global transcription termination control system for methionine and cysteine biosynthesis genes in gram-positive bacteria. *Mol Microbiol* 30: 737–749
- Hanson TE and Tabita FR (2001) A ribulose-1,5-bisphosphate carboxylase/oxygenase (Rubisco)-like protein from *Chlorobium tepidum* that is involved with sulfur metabolism and the response to oxidative stress. *Proc Natl Acad Sci USA* 98: 4397–4402
- Ide T, Baumer S and Deppenmeier U (1999) Energy conservation by the H₂:heterodisulfide oxidoreductase from *Methanosarcina mazei* G01: identification of two proton-translocating segments. *J Bacteriol* 181: 4076–4080
- Kim KK, Kim R and Kim SH (1998) Crystal structure of a small heat-shock protein. *Nature* 394: 595–599
- King KY, Horenstein JA and Caparon MG (2000) Aerotolerance and peroxide resistance in peroxidase and PerR mutants of *Streptococcus pyogenes*. *J Bacteriol* 182: 5290–5299
- Markwell MA, Haas SM, Bieber LL and Tolbert NE (1978) A modification of the Lowry procedure to simplify protein determination in membrane and lipoprotein samples. *Anal Biochem* 87: 206–210
- Mitsumoto A, Takeuchi A, Okawa K and Nakagawa Y (2002) A subset of newly synthesized polypeptides in mitochondria from human endothelial cells exposed to hydroperoxide stress. *Free Radic Biol Med* 32: 22–37
- Mongkolsuk S, Praituan W, Loprasert S, Fuangthong M and Chamnongpol S (1998) Identification and characterization of a new organic hydroperoxide resistance (*ohr*) gene with a novel pattern of oxidative stress regulation from *Xanthomonas campestris* pv. *phaseoli*. *J Bacteriol* 180: 2636–2643
- Mukhopadhyay B, Johnson E and Ascano M (1999) Conditions for vigorous growth on sulfide and reactor-scale cultivation protocols for the thermophilic green sulfur bacterium *Chlorobium tepidum*. *Appl Environ Microbiol* 65: 301–306
- Murphy BA, Grundy FJ and Henkin TM (2002) Prediction of gene function in methylthioadenosine recycling from regulatory signals. *J Bacteriol* 184: 2314–2318
- Page RD (1996) TreeView: an application to display phylogenetic trees on personal computers. *Comput Appl Biosci* 12: 357–358
- Paschinger H, Paschinger J and Gaffron H (1974) Photochemical disproportionation of sulfur into sulfide and sulfate by *Chlorobium limicola* forma *thiosulfatophilum*. *Arch Microbiol* 96: 341–351
- Pott AS and Dahl C (1998) Sirohaem sulfite reductase and other proteins encoded by genes at the *dsr* locus of *Chromatium vinosum* are involved in the oxidation of intracellular sulfur. *Microbiology* 144: 1881–1894
- Quentmeier A and Friedrich CG (2001) The cysteine residue of the SoxY protein as the active site of protein-bound sulfur oxidation of *Paracoccus pantotrophus* GB17. *FEBS Lett* 503: 168–172
- Rince A, Giard JC, Pichereau V, Flahaut S and Auffray Y (2001) Identification and characterization of gsp65, an organic hydroperoxide resistance (*ohr*) gene encoding a general stress protein in *Enterococcus faecalis*. *J Bacteriol* 183: 1482–1488
- Rother D, Henrich HJ, Quentmeier A, Bardischewsky F and Friedrich CG (2001) Novel genes of the *sox* gene cluster, mutagenesis of the flavoprotein SoxF, and evidence for a general sulfur-oxidizing system in *Paracoccus pantotrophus* GB17. *J Bacteriol* 183: 4499–4508
- Saibil H (2000) Molecular chaperones: containers and surfaces for folding, stabilising or unfolding proteins. *Curr Opin Struct Biol* 10: 251–258
- Sekowska A and Danchin A (2002) The methionine salvage pathway in *Bacillus subtilis*. *BMC Microbiol* 2: 8.
- Setzke E, Hedderich R, Heiden S and Thauer RK (1994) H₂:heterodisulfide oxidoreductase complex from *Methanobacterium thermoautotrophicum*. Composition and properties. *Eur J Biochem* 220: 139–148
- Shahak Y, Arieli B, Padan E and Hauska G (1992) Sulfide quinone reductase (SQR) activity in *Chlorobium*. *FEBS Lett* 299: 127–130
- Sherman M and Goldberg A (1992) Heat shock in *Escherichia coli* alters the protein-binding properties of the chaperonin *groEL* by inducing its phosphorylation. *Nature* 357: 167–169
- Soto A, Allona I, Collada C, Guevara MA, Casado R, Rodríguez-Cerezo E, Aragoncillo C and Gomez L (1999) Heterologous expression of a plant small heat-shock protein enhances *Escherichia coli* viability under heat and cold stress. *Plant Physiol* 120: 521–528
- Sun W, Bernard C, van de Cotte B, Van Montagu M and Verbruggen N (2001) At-HSP17.6A, encoding a small heat-shock protein in *Arabidopsis*, can enhance osmotolerance upon overexpression. *Plant J* 27: 407–415
- Tabita F (1999) Microbial ribulose-1,5-bisphosphate carboxylase/oxygenase: a different perspective. *Photosynth Res* 60: 1–28
- Takemoto T, Zhang QM and Yonei S (1998) Different mechanisms of thioredoxin in its reduced and oxidized forms in defense against hydrogen peroxide in *Escherichia coli*. *Free Radic Biol Med* 24: 556–562
- Thompson JD, Gibson TJ, Plewniak F, Jeanmougin F and Higgins DG (1997) The CLUSTAL_X windows interface: flexible strategies for multiple sequence alignment aided by quality analysis tools. *Nucleic Acids Res* 25: 4876–4882
- Tong S, Porco A, Isturiz T and Conway T (1996) Cloning and molecular genetic characterization of the *Escherichia coli* *gntR*, *gntK*, and *gntU* genes of GntI, the main system for gluconate metabolism. *J Bacteriol* 178: 3260–3269

- Truper HG and Schlegel HG (1964) Sulphur metabolism in *Thiorhodaceae* I. Quantitative measurements in growing cells of *Chromatium okenii*. *Antonie van Leeuwenhoek* 30: 225–238
- Vassilieva EV, Stirewalt VL, Jakobs CU, Frigaard N-U, Inoue-Sakamoto K, Baker MA, Sotak A and Bryant DA (2002) Subcellular localization of chlorosome proteins in *Chlorobium tepidum* and characterization of three new chlorosome proteins: CsmF, CsmH, and CsmX. *Biochemistry* 41: 4358–4370
- Verte F, Kostanjevecki V, De Smet L, Meyer TE, Cusanovich MA and Van Beeumen JJ (2002) Identification of a thiosulfate utilization gene cluster from the green phototrophic bacterium *Chlorobium limicola*. *Biochemistry* 41: 2932–2945
- Wahlund TM and Madigan MT (1995) Genetic transfer by conjugation in the thermophilic green sulfur bacterium *Chlorobium tepidum*. *J Bacteriol* 177: 2583–2588
- Wahlund TM, Woese CR, Castenholz RW and Madigan MT (1991) A thermophilic green sulfur bacterium from New Zealand hot springs, *Chlorobium tepidum* sp-nov. *Arch Microbiol* 156: 81–90
- Waters ER (1995) The molecular evolution of the small heat-shock proteins in plants. *Genetics* 141: 785–795
- Watson GMF, Yu J-P and Tabita FR (1999) Unusual ribulose 1,5-bisphosphate carboxylase/oxygenase of anoxic archaea. *J Bacteriol* 181: 1569–1575
- Westley J (1987) Thiocyanate and thiosulfate. *Meth Enzymol* 143: 22–25
- Wodara C, Kostka S, Egert M, Kelly DP and Friedrich CG (1994) Identification and sequence analysis of the *soxB* gene essential for sulfur oxidation of *Paracoccus denitrificans* GB17. *J Bacteriol* 176: 6188–6191
- Yamamoto Y, Higuchi M, Poole LB and Kamio Y (2000) Role of the *dpr* product in oxygen tolerance in *Streptococcus mutans*. *J Bacteriol* 182: 3740–3747
- Zhu Z, Sun D and Davidson VL (1999) Localization of periplasmic redox proteins of *Alcaligenes faecalis* by a modified general method for fractionating gram-negative bacteria. *J Bacteriol* 181: 6540–6542